

RESEARCH ARTICLE

A particle filter for ammonia coverage ratio and input simultaneous estimations in Diesel-engine SCR system

Kangfeng Sun, Fenzhu Ji, Xiaoyu Yan, Kai Jiang, Shichun Yang*

School of Transportation Science and Engineering, Beihang University, Beijing, China

* yangshichun@buaa.edu.cn



Abstract

As NO_x emissions legislation for Diesel-engines is becoming more stringent than ever before, an aftertreatment system has been widely used in many countries. Specifically, to reduce the NO_x emissions, a selective catalytic reduction(SCR) system has become one of the most promising techniques for Diesel-engine vehicle applications. In the SCR system, input ammonia concentration and ammonia coverage ratio are regarded as essential states in the control-oriental model. Currently, an ammonia sensor placed before the SCR Can is a good strategy for the input ammonia concentration value. However, physical sensor would increase the SCR system cost and the ammonia coverage ratio information cannot be directly measured by physical sensor. Aiming to tackle this problem, an observer based on particle filter(PF) is investigated to estimate the input ammonia concentration and ammonia coverage ratio. Simulation results through the experimentally-validated full vehicle simulator cX-Emission show that the performance of observer based on PF is outstanding, and the estimation error is very small.

OPEN ACCESS

Citation: Sun K, Ji F, Yan X, Jiang K, Yang S (2018) A particle filter for ammonia coverage ratio and input simultaneous estimations in Diesel-engine SCR system. PLoS ONE 13(2): e0192217. <https://doi.org/10.1371/journal.pone.0192217>

Editor: Xiaosong Hu, Chongqing University, CHINA

Received: October 10, 2017

Accepted: January 19, 2018

Published: February 6, 2018

Copyright: © 2018 Sun et al. This is an open access article distributed under the terms of the [Creative Commons Attribution License](https://creativecommons.org/licenses/by/4.0/), which permits unrestricted use, distribution, and reproduction in any medium, provided the original author and source are credited.

Data Availability Statement: All relevant data are within the paper and its Supporting Information files.

Funding: This work is supported by National Natural Science Foundation of China, (<http://www.nsf.gov.cn>), grant number: 51576011 to SCY. The funder had no role in study design, data collection and analysis, decision to publish, or preparation of the manuscript.

Competing interests: The authors have declared that no competing interests exist.

Introduction

In recent years, a phenomenon is that Diesel-engines have got more attentions due to their excellent fuel efficiency and lower greenhouse emissions compared with gasoline counterparts [1]. And Diesel-engines are quite important for the conventional and electrified vehicles in the future[2]. However, the Diesel-engine flame temperatures are high, which lead to the oxidation of nitrogen into NO_x[3, 4]. The emissions of NO_x would result to ozone depletion, acid rain and photochemical smog formation, which do harm to the environment and human health[4, 5]. To avoid NO_x emissions, the legislation for Diesel-engines emissions is becoming increasingly stringent than ever before. In order to meet with the current and proposed emission regulations, many efforts have been paid to deal with the high-NO_x emissions problems[6]. It is known that only employing combustion control strategies such as variable valve actuation system(VVA), exhaust gas recirculation(EGR) etc. cannot meet the stringent emission regulations[5, 7, 8]. Therefore, some types of aftertreatment systems including the diesel oxidation catalyst(DOC), the diesel particle filter(DPF), and the selective catalytic reduction(SCR)

systems are widely used in the Diesel-engines. Specifically, the main function of the DOC system is to oxidize the un-burned hydrocarbon and the carbon monoxide. The DPF device is used to capture the PM. The SCR component has the ability to convert the NO_x emissions into nitrogen (N₂) and water (H₂O) which are friendly to the environment and human health. Among all types of aftertreatment systems, pointed in Ref. [9], the urea-based SCR system has been proved one of the most promising techniques to reduce NO_x emissions and fulfill NO_x emissions standards for Diesel-engine vehicle applications in the future.

In the urea-based SCR system, the primary principle is to spray urea solution into the exhaust pipe before the SCR tank. Under the high temperature exhaust condition, the injected urea solution can be converted into gaseous ammonia which is then absorbed on the catalyst surface and reacts with NO_x[10]. Generally speaking, higher urea injection would lead to higher NO_x conversion and less NO_x emissions in the tailpipe[3]. However, if the urea is overdosed than the NO_x emissions, the gaseous ammonia would slip into the tailpipe which is also harmful to the environment and human health. Thus, the urea dosing closed-loop control, aiming to achieve a high NO_x conversion and low ammonia slip, of the SCR system, is proposed[11]. Many studies on the urea dosage control can be seen in[12, 13].

Among the SCR closed-loop control strategies, the input ammonia concentration and the ammonia coverage ratio are considered as the critical states in the construction of the feedback control strategy[2, 14]. To obtain the input ammonia concentration information, a physical sensor placed at the inlet of the SCR system is utilized to measure the concentration value. However, on one hand, the physical commercial sensors would increase the SCR cost and diagnosis challenge[15, 16]. On the other hand, there is no commercial sensor to measure the ammonia coverage ratio directly[3]. To deal with this problem, a promising strategy is to design an observer to estimate the input ammonia concentration and ammonia coverage ratio information. In order to develop the observer, there are considerable methods. The well-known strategies include the Kalman filter(KF)[17] and the Luenberger observer[18] which have been successfully applied to many fields of science and engineering. However, both methods are suitable for linear systems. It is important to note that the chemical processes in the SCR tank are complex and the approximated SCR model exhibits strong nonlinear dynamics and possible non-Gaussian noise[9, 19]. Therefore, how to develop an observer that provides an exact optimal solution to the SCR system remains an open problem. Though the modified KF, also known as extended Kalman filter(EKF), is the most traditional estimator for nonlinear systems, it has been demonstrated to perform poorly in the non-Gaussian posterior estimates obtained when the system is nonlinear[20]. The EKF requires that the nonlinear state transition equations and measurement equations are approximated to linear equations by using the first-order Taylor series expansion, so that the KF can be applied to estimate the states. Moreover, it requires the nonlinearity of the model is small and the deviation of the approximation is not big[20], which is however not exhibited by the SCR system that involves complicate chemical reaction processes and time-varying reaction conditions. Therefore, though the EKF works well in many cases, an alternate observer needs to be developed to provide a better estimation in the SCR system. To address the uncertainties especially in strong nonlinear and non-Gaussian systems, particle filter(PF) algorithm has been given relatively more efforts. Unlike the EKF, PF relies on fitting an approximate solution to the nonlinear equation rather than solving the linear equations obtained by approximating the nonlinear system[20]. It makes use of the Bayesian filter and Monte Carlo method to estimate the states. The state distribution is represented by a set of random samples with associated weights. High probability density is represented by a huge number of particles, low probability by a low number or no particles[20]. It refers from many researchers that for strong nonlinear and non-Gaussian systems, if the model is not accurate enough, then the PF algorithm is considered very useful to

do the state estimation[21, 22]. A well-studied applications of PF is the lithium-ion battery system, where PFs were used for the state estimation such as state-of-health, state of charge, remaining useful life, etc.[23–25]. Therefore, in order to deal with the strong nonlinear dynamics and possible strong non-Gaussian noise in the SCR system, we aim to design an observer based on the PF to estimate both ammonia inputs and coverage ratio at the same time.

In this paper, we propose a technique by using the PF to simultaneously estimate the ammonia input and ammonia coverage ratio. As a contrast, an observer based on the EKF is also designed. The contributions and novelty of the work can be summarized as: (1) Considering the strong nonlinearity, it aims to propose the PF algorithm for the SCR system. (2) Based on the PF, the observer is designed to estimate the ammonia coverage ratio which is a crucial state and cannot be directly measured by physical sensors, and the input ammonia concentration is estimated such that the urea-to-ammonia rate is available without mounting an extra ammonia sensor at the entrance of the SCR tank. (3) The proposed PF observer is verified by using the data from an experimentally-validated full vehicle simulator cX-Emission. The comparisons show the advantage of the proposed PF observer over the traditional EKF observer.

The rest of this paper is organized as follows. A concise introduction of the SCR reaction model is shown in section 2. Then an observer model for state estimation is designed in section 3. In section 4, the simulation results are presented to verify the performance of the proposed technique. At last, concluding remarks are summarized in section 5.

Selective catalytic reduction(SCR)

2.1. SCR operation principle

The main function of a SCR system is to catalytically convert the engine-out NO_x into nitrogen and water, and consequently, reduce the NO_x emissions in the exhaust tailpipe of a Diesel-engine. Therefore, in the urea-based SCR system, the 32.5% aqueous urea solution is injected into the upstream exhaust pipe. The schematic diagram of a SCR system is shown in Fig 1. Generally speaking, the NO_x reduction mainly consists of three parts. (1) urea solution sprayed into the exhaust pipe is converted into ammonia through a certain number of processes including the evaporation of urea solution, thermal decomposition of pure urea, and the hydrolyzation of isocyanic acid. Then, the gaseous ammonia flows into upstream of the SCR device. (2) most of the ammonia is absorbed on the surface of the catalyst. Meanwhile, the absorbed ammonia is partly desorbed from the surface. (3) the absorbed ammonia reacts with NO_x and converts it into nitrogen and water[26, 27].

The chief chemical reactions and corresponding reaction rate equations are summarized as follows:

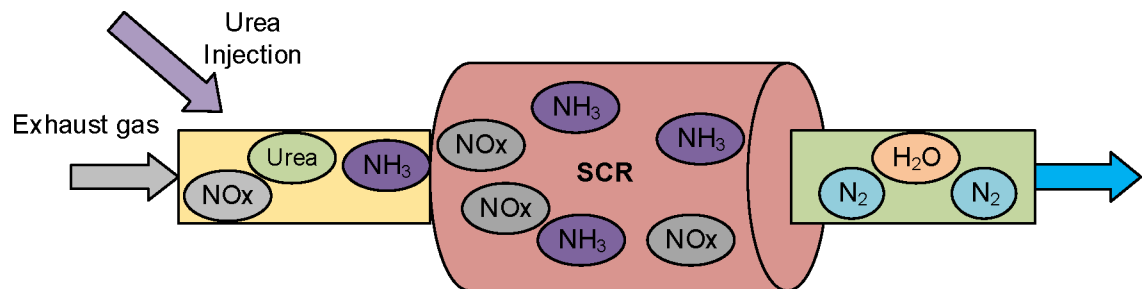
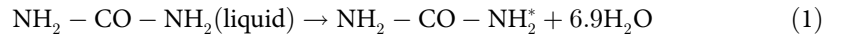


Fig 1. Schematic diagram of SCR system.

<https://doi.org/10.1371/journal.pone.0192217.g001>

- (1) Urea evaporation: the urea solution evaporates into solid phase of urea under the ideal situation. The reaction is represented as follows:

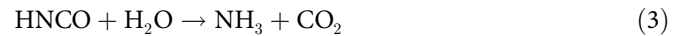


where $\text{NH}_2 - \text{CO} - \text{NH}_2^*$ expresses the pure urea.

- (2) Urea decomposition: solid urea is decomposed into ammonia and equimolar amount of isocyanic acid when the exhaust gas temperature is sufficiently high. The reaction is shown as follows:



- (3) Isocyanic acid hydrolyzation: in this part, the isocyanic acid is hydrolyzed to ammonia and carbon dioxide. The reaction is described as follows:



- (4) Adsorption/desorption: the ammonia in the catalytic tank is adsorbed on the SCR substrate, and the adsorbed ammonia can also be desorbed from the substrate. The reversible reaction is represented as follows:



Where θ_{free} is the free SCR catalyst site, and the NH_3^* refers to the NH_3 adsorbed on the SCR substrate which is ready to react with NOx; the forward direction describes the adsorption process while the reverse direction denotes the desorption process.

The rate of the reversible reaction can be shown as follows[28]:

$$R_{\text{ad}} = K_{\text{ad}} \exp\left(-\frac{E_{\text{ad}}}{RT}\right) C_{\text{NH}_3} (1 - \theta_{\text{NH}_3}) \quad (5)$$

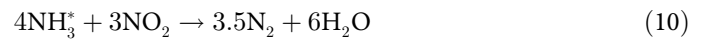
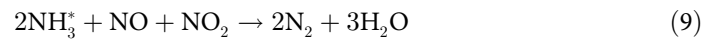
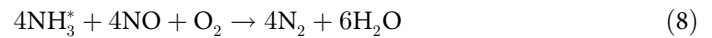
$$R_{\text{de}} = K_{\text{de}} \exp\left(-\frac{E_{\text{de}}}{RT}\right) C_{\text{NH}_3} \theta_{\text{NH}_3} \quad (6)$$

where R_x represents the rate of the chemical reaction; T is temperature; E , K , and R are constants; C_x expresses concentration of x , and θ_{NH_3} is the ammonia coverage ratio, which is defined as:

$$\theta_{\text{NH}_3} = \frac{M_{\text{NH}_3}^*}{\Theta} \quad (7)$$

where $M_{\text{NH}_3}^*$ indicates the number of moles of the ammonia adsorbed on the SCR substrate. Θ expresses the ammonia storage capacity which depends on the exhaust temperature.

(5) NOx reduction: the chief reduction reactions can be described as follows:



Among the Diesel-engine exhaust NOx, NO is more than 90%, and the reaction rate of Eq (8) is quite fast. Therefore, in the SCR reaction tank, the dominant reduction reaction is Eq (8). The relevant reaction rate is shown as follows:

$$R_{re} = K_{re} \exp\left(-\frac{E_{re}}{RT}\right) C_{\text{NO}} \theta_{\text{NH}_3} \quad (11)$$

(6) Ammonia oxidation: if the temperature is more than 450°C, the adsorbed NH₃ would be oxidized to NO. The reaction equation can be proposed as follows:



The reaction rate is presented as below:

$$R_{ox} = K_{ox} \exp\left(-\frac{E_{ox}}{RT}\right) \theta_{\text{NH}_3} \quad (13)$$

2.2. SCR model

In this work, we suppose that the SCR reaction device is a Continuously Stirred Tank Reactor (CSTR). Based on the above chemical reactions, molar balance and the conservation of mass, the dynamic equation of SCR system can be established as follows.

$$\dot{C}_{\text{NO}} = \Theta(R_{ox} - R_{re}) \quad (14)$$

$$\dot{\theta}_{\text{NH}_3} = R_{ad} - R_{de} - R_{re} - R_{ox} \quad (15)$$

$$\dot{C}_{\text{NH}_3} = \Theta(R_{de} - R_{ad}) \quad (16)$$

In the literature, there are many SCR models for ground vehicle applications such as the four-state model in [29], and five-state model in [10]. Generally speaking, four states or more states model may describe the actual SCR system better. However, with four or more states, the model designing and parameter identification would be more complicated. What's more, to design controllers, detect fault and monitor system, more sensors and observers are also needed [30]. Therefore, considering the model accuracy and the project cost, a three-state non-linear model is developed as below, which has been validated by Diesel-engine aftertreatment

experiments[31, 32]:

$$\begin{bmatrix} \dot{C}_{NO} \\ \dot{\theta}_{NH_3} \\ \dot{C}_{NH_3} \end{bmatrix} = \begin{bmatrix} -C_{NO} \left(\Theta r_{re} \theta_{NH_3} + \frac{F}{V} \right) + r_{ox} \Theta \theta_{NH_3} \\ -\theta_{NH_3} (r_{ad} C_{NH_3} + r_{de} + r_{re} C_{NO} + r_{ox}) + r_{ad} C_{NH_3} \\ -C_{NH_3} \left[\Theta r_{ad} (1 - \theta_{NH_3}) + \frac{F}{V} \right] + r_{de} \Theta \theta_{NH_3} \end{bmatrix} + \begin{bmatrix} 0 \\ 0 \\ \frac{F}{V} \end{bmatrix} C_{NH_3,in} + \begin{bmatrix} \frac{F}{V} \\ 0 \\ 0 \end{bmatrix} C_{NO,in} \tag{17}$$

where $r_x = K_x \exp\left(-\frac{E_x}{RT}\right)$, x denotes ad, de, ox, re; C_{NO} and C_{NH_3} represent the NOx and ammonia concentration in the tailpipe; $C_{NH_3,in}$ and $C_{NO,in}$ indicates the inlet ammonia and NOx concentration respectively. F is the exhaust gas flow rate; V is the volume of the SCR Can.

Observer design for ammonia input and coverage ratio estimations

In appropriate SCR controllers, input concentrations, state information, output concentrations and temperature are necessary. In general, two ammonia sensors, two NOx sensors and one temperature sensor are mounted in the SCR device to measure the essential parameters. The schematic diagram of the SCR system and location of sensors are presented in Fig 2(A). Actually, the physical sensors are expensive and too many sensors would increase the SCR cost and diagnosis challenge. Moreover, there is no commercial sensor to measure the ammonia coverage ratio directly which is a crucial state in the construction of the feedback control strategy. Thus, it is necessary to design an observer to estimate the ammonia coverage ratio and input ammonia concentration. The architecture diagram of the observer designed in this work is shown in Fig 2(B) which estimates the ammonia coverage ratio and reduces an ammonia sensor at the entrance of the SCR tank.

In order to develop the observer, there are considerable methods. Considering the system nonlinearities and measurement noises, the EKF algorithm is the most classic and widely-used method. However, the method requires that the linearization of the nonlinear model to which the KF can be applied keeps small deviation, the nonlinearity of the model is not big and the noise is Gaussian or independent and identically distributed which are hard to satisfy in the SCR system [19, 20]. Therefore, the observer based on EKF algorithm may not perform well in the state estimation of the SCR system. Considering the strong uncertainties in the SCR system, PF algorithm is a novel filtering method which fits on an approximate solution to the nonlinear model rather than solving the linear model obtained by approximating the nonlinear system[20, 33]. More importantly, PF algorithm should have notably better estimation accuracy than EKF approach. It makes use of the recursive Bayesian filtering of Monte Carlo simulations towards state estimation and makes no restriction to the state space models and the distribution of the noise.

In our study, the traditional EKF and PF have been used to estimate the ammonia input concentration and coverage ratio. The algorithms for the two observers are described in the following sections. Then the state space model for observer is presented.

3.1. The EKF algorithm

The EKF algorithm is the most widely used state estimation technique in nonlinear system which uses a linearized model and KF algorithm at each sample time. The nonlinear system

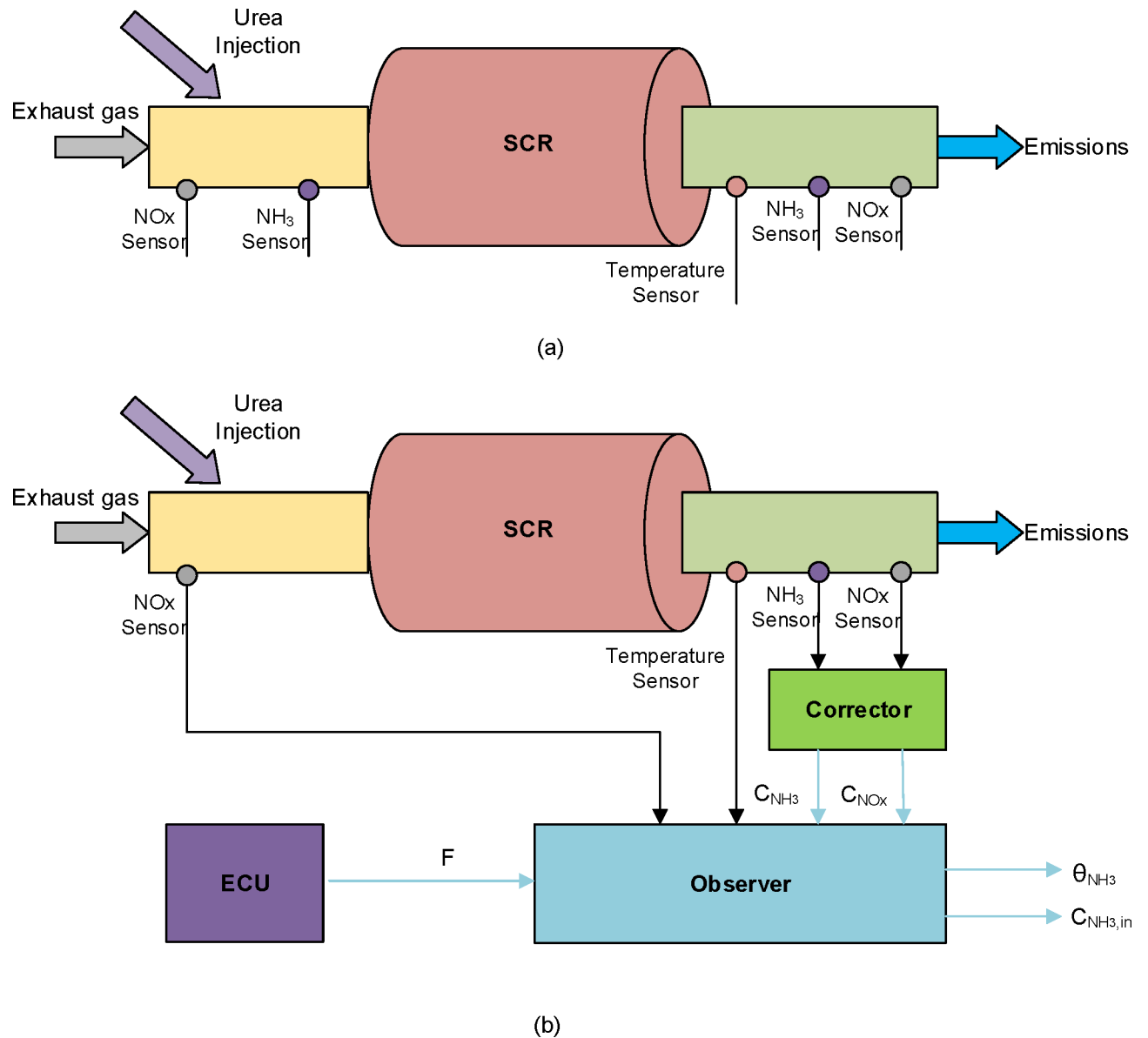


Fig 2. Schematic diagram of SCR system with corresponding sensors (a) and with observer architecture diagram (b).

<https://doi.org/10.1371/journal.pone.0192217.g002>

can be described as below:

$$x_k = f[x_{k-1}, u_k] + w_k \quad (18)$$

$$z_k = h[x_k] + v_k \quad (19)$$

where x_k and u_k is the state vector and input vector respectively, $f(x)$ expresses the relevant prediction function, w_k denotes the process noise whose covariance is Q_k . In (19), $h(x)$ is the measurement function, the corresponding noise and noise covariance are v_k and R_k respectively.

Following a linearization procedure of Eq (18) and Eq (19), linear state space form to which KF can be applied is obtained as follows:

$$x_{k+1} = A_k x_k + B_k U_k + w_k \tag{20}$$

$$z_k = H_k x_k + v_k \tag{21}$$

Then the EKF recursion can be summarized below.

- (1) Prediction step: the priori estimations of the state vector x_k and the system error covariance P_k are obtained as follows.

$$\hat{x}_k^- = f(\hat{x}_{k-1}, u_{k-1}) \tag{22}$$

$$P_k^- = A_{k-1} P_{k-1} A_{k-1}^T + Q \tag{23}$$

- (2) Calculate the Kalman gain: the Kalman gain defines the extent to which the observer trust the state estimate or measurement[20].

$$K_k = P_k^- H_k^T (H_k P_k^- H_k^T + R)^{-1} \tag{24}$$

- (3) Measurement update step: calculate the posteriori estimations of the state vector and error covariance using the measurement information.

$$\hat{x}_k = \hat{x}_k^- + K_k (z_k - h(\hat{x}_k^-)) \tag{25}$$

$$P_k = P_k^- - K_k H_k P_k^- \tag{26}$$

3.2. The PF algorithm

Unlike the EKF which requires the linearization of the nonlinear system, the PF algorithm does not require that the system is linear or Gaussian distributed by using the Bayesian filter and Monte Carlo approach. This method begins with a set of random particles which are then propagated through the state transition equation to obtain priori particles. Then, the available measurement information is fused with these priori particles to give posteriori distribution. An excellent tutorials of PF can be seen in [34]. For a nonlinear system described in Eq (18) and Eq (19), the PF algorithm can be performed in 3 steps.

- (1) Initialization: a set of random particles $x_{0,i}$ ($i = 1, 2, \dots, N$) are generated based on the initial pdf of $p(x_0)$.
- (2) Importance sampling: the randomly generated particles are propagated through the state transition equation Eq (18) to obtain the priori distribution particles with the importance

weight q_i which can be calculated as follows.

$$x_{k,i}^- = f(x_{k-1,i}, u_{k-1}) + w_{k-1} \quad (i = 1, 2, \dots, N) \tag{27}$$

$$q_i = p\langle (z_k = z^*) | (x_k = x_{k,i}^-) \rangle = p\left[v_k = z^* - h(x_{k,i}^-) \right] \\ \approx \frac{1}{(2\pi)^{m/2} |R|^{1/2}} \exp\left(\frac{-[z^* - h(x_{k,i}^-)]^T R^{-1} [z^* - h(x_{k,i}^-)]}{2} \right) \tag{28}$$

$$q_i = \frac{q_i}{\sum_{j=1}^N q_j} \tag{29}$$

where z^* indicates the measurement value.

- (3) Resampling: resampling approach are made to reduce the degeneracy phenomena during the iteration. After resampling, the particles with large weight are replicated and particles with small weight are discarded[33]. There are several methods to make resampling, such as systematic resampling, multinational resampling, residual sampling, etc.[35]. In this paper, the systematic resampling

3.3. Ammonia input and coverage ratio estimations

Since the system model is built and the necessary parameters can be measured by physical sensors, the input ammonia concentration and ammonia coverage ratio can be estimated by EKF and PF described above. As the ammonia concentration varies very slowly over time, then, the derivative of input ammonia concentration can be assumed as zero[30]:

$$\dot{C}_{NH_3, in} = 0 \tag{30}$$

The state space model in discrete form for input ammonia concentration and ammonia coverage ratio predictions are built as follows:

$$\hat{x}(k|k-1) = \begin{bmatrix} \hat{\theta}_{NH_3}(k|k-1) \\ \hat{C}_{NH_3, in}(k|k-1) \end{bmatrix} = f[\hat{x}(k-1|k-1)] = \begin{bmatrix} \hat{\theta}_{NH_3}(k-1|k-1) + -\Delta T \dot{\hat{\theta}}_{NH_3}(k|k-1) \\ \hat{C}_{NH_3, in}(k-1|k-1) \end{bmatrix} \tag{31}$$

where ΔT is the updating time of the PF model.

The post NOx sensor and ammonia sensor reading are selected for the measurement equation which can be shown as follows:

$$z(k) = h[\hat{x}(k)] = \begin{bmatrix} C_{NO}(k) \\ C_{NH_3}(k) \end{bmatrix} = \begin{bmatrix} \hat{C}_{NO}(k-1) + \frac{1}{2} - \Delta T [\dot{\hat{C}}_{NO}(k) + \dot{\hat{C}}_{NO}(k-1)] \\ \hat{C}_{NH_3}(k-1) + \frac{1}{2} - \Delta T [\dot{\hat{C}}_{NH_3}(k) + \dot{\hat{C}}_{NH_3}(k-1)] \end{bmatrix} \tag{32}$$

where

$$\dot{\hat{C}}_{NO}(k) = -C_{NO} \left[\Theta_{r_{re}} \hat{\theta}_{NH_3}(k|k-1) + \frac{F}{V} \right] + r_{ox} \Theta \hat{\theta}_{NH_3}(k|k-1) + \frac{F}{V} C_{NO, in} \tag{33}$$

$$\begin{aligned} \dot{\hat{C}}_{\text{NH}_3}(k) = & -C_{\text{NH}_3} \left[\Theta r_{\text{ad}} \left(1 - \hat{\theta}_{\text{NH}_3}(k|k-1) \right) + \frac{F}{V} \right] + r_{\text{dc}} \Theta \hat{\theta}_{\text{NH}_3}(k|k-1) \\ & + \frac{F}{V} \hat{C}_{\text{NH}_3, \text{in}}(k|k-1) \end{aligned} \quad (34)$$

where $C_{\text{NO}, \text{in}}$ is the NOx input concentration value measured by physical NOx sensor placed before the SCR Can.

Remarks: In the observer designed, two NOx sensors placed at the entrance of the SCR Can and the tailpipe respectively are needed and one ammonia sensor located at the tailpipe is also necessary. It is worth noting that most onboard NOx sensors have significant ammonia cross sensitivity which would make the observation unsatisfactory if the inaccurate NOx sensor reading is used. However, by using the measurement value of ammonia sensor and temperature sensor in the tailpipe, the NOx sensor reading can be corrected to eliminate the effect of gaseous ammonia species. In recent years, a lot of approaches have been proposed to obtain the corrected NOx sensor [36, 37]. In this paper, a temperature-dependent cross-sensitivity factor is used to correct the NOx sensor values.

Simulation results and comparisons

The parameters of the SCR system model established above are derived from the previous research results in [38]. With these identified parameters, the PF observer is designed and the simulations and comparisons are carried out based on an experimentally-validated full vehicle simulator cX-Emission exploited by the Center for Automotive Research at the Ohio State University [12]. The full vehicle simulator cX-Emission is developed by using the Model-Based Design in MATLAB/Simulink and the architecture of the developed full vehicle simulator is selected that utilizes a 1.9 L Diesel-engine belted to a 10.6kW starter/alternator; see Ref [39].

For the simulation, as we can see in the SCR system model in Eq (17), the exhaust gas flow rate, exhaust temperature and engine-out NOx concentration are all required. For these information, the city driving cycle FTP-75 is used which is a test cycle released by the US Environmental Protection Agency (EPA) to measure the tailpipe emissions and fuel economy. According to the cX-Emission simulator and the FTP-75 test cycle, the exhaust flow rate, exhaust temperature, engine-out NOx concentration and input ammonia concentration of SCR system during the test are presented as follows.

Fig 3 shows the exhaust gas flow rate and temperature during the FTP-75 test cycle. We can see that the flow rate and temperature vary a lot which is representative for the real-world applications. Fig 4 depicts the engine-out NOx concentration which is the sum of the NO and NO₂ concentrations. The model predicted tailpipe NOx and ammonia concentration are presented in Fig 5. Compared with the engine-out NOx concentration, the tailpipe NOx concentration does not decrease significantly, that is because the temperature is low, the reduction rate is slow. The exhaust temperature is low in the period of 110s to 160s, resulting in no urea injection in order to avoid urea crystallization, and this also leads to a significant reduction in the concentration of tailpipe ammonia.

As above-presented, the designed input ammonia concentration and ammonia coverage ratio observer based on PF is simulated based on the selected FTP-75 cycle. Fig 6 depicts the input ammonia concentration comparison during the test. The solid-blue line is the input ammonia concentration which is obtained based on the PID control law in [40]. The red and pink curve shows the estimated ammonia concentration by the designed EKF and PF observer respectively. As can be seen from Fig 6, the observations quickly respond to the calculated

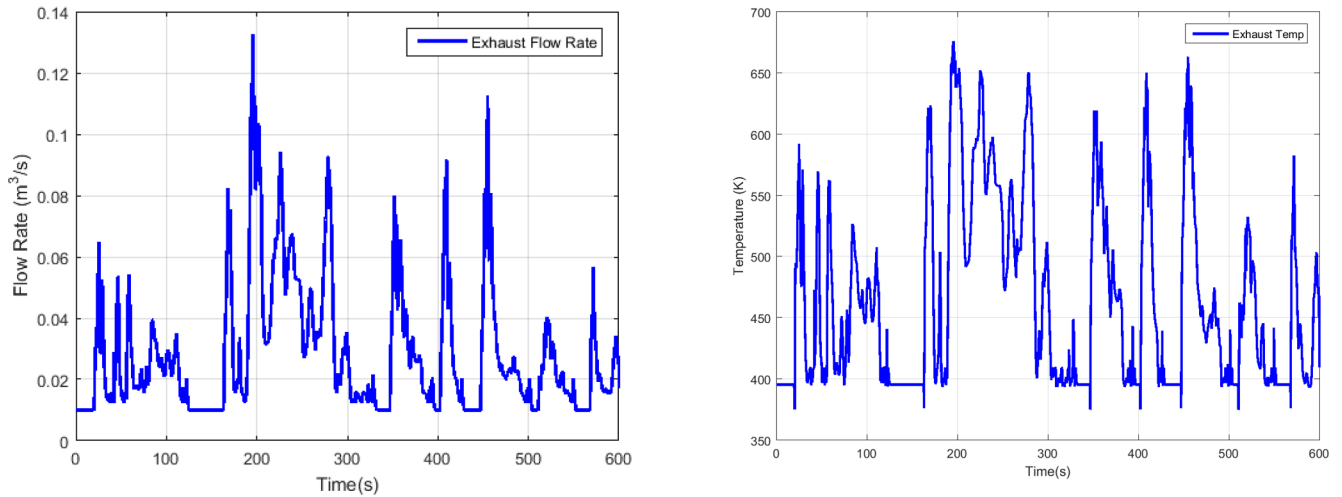


Fig 3. Exhaust flow rate and exhaust temperature during the FTP-75 test cycle simulation.

<https://doi.org/10.1371/journal.pone.0192217.g003>

values of the SCR model and has a good traceability where the calculated values change. Fig 7 shows the errors between the observer estimation and the SCR model predicted value. The error is defined as the model predicted value minus the observer estimated value. However, compared with EKF-based observer, as shown in Fig 7, the PF observer get the smaller errors which are quite small being of the order of 10^{-4} . Therefore, as expected, we can claim that the

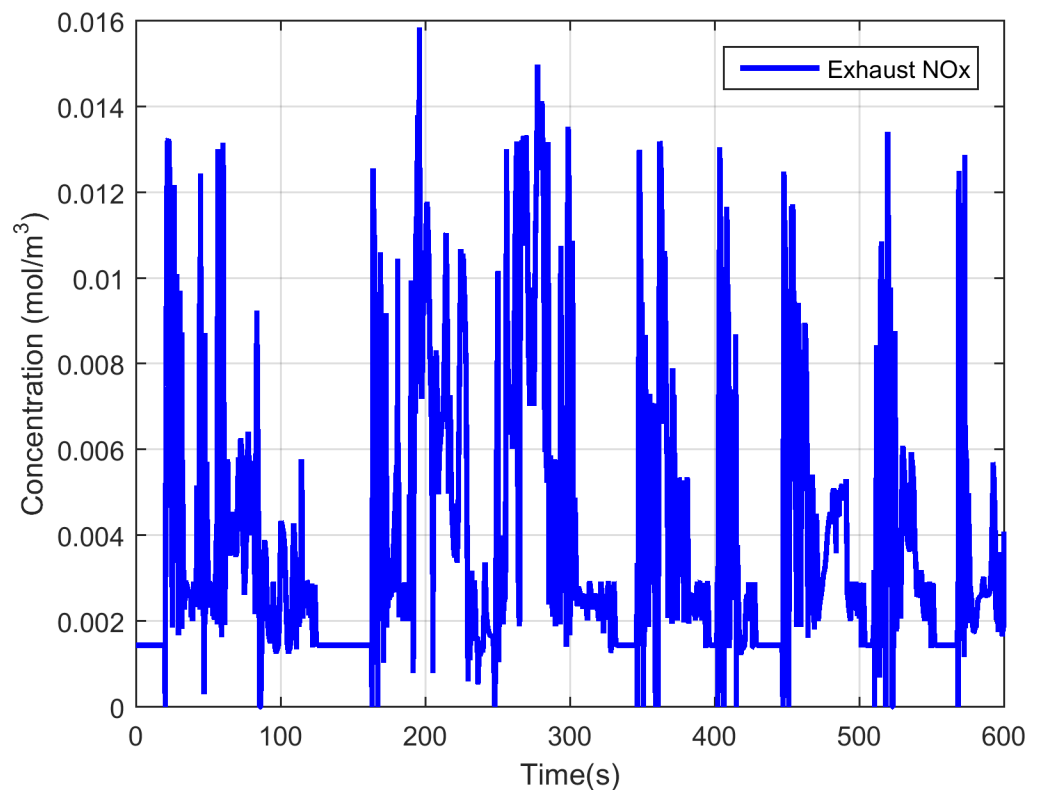


Fig 4. The engine-out NOx concentration during the FTP-75 test cycle simulation.

<https://doi.org/10.1371/journal.pone.0192217.g004>

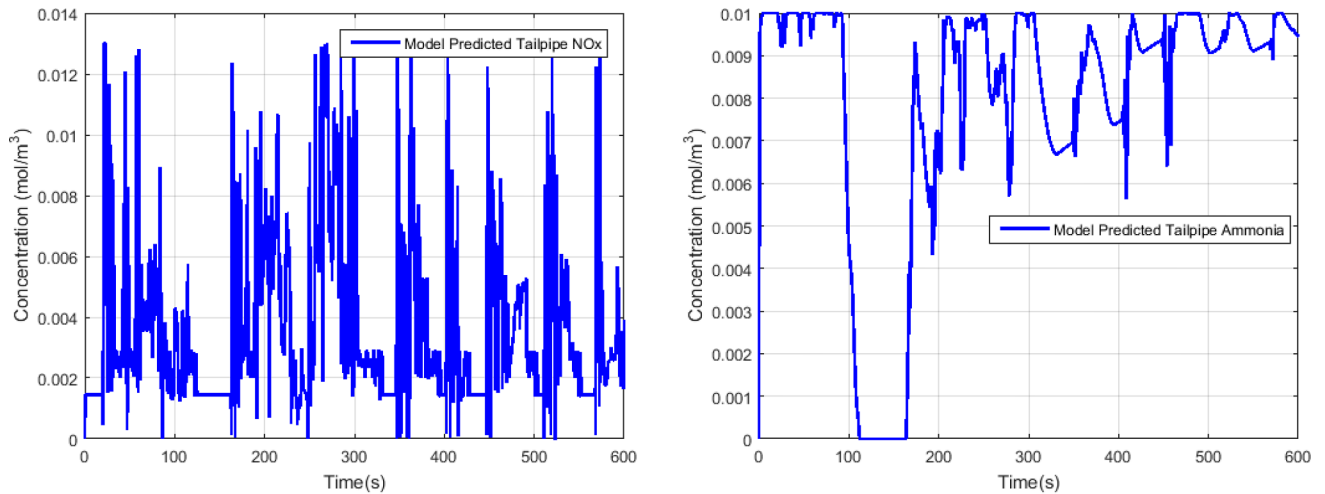


Fig 5. The model predicted tailpipe NOx and ammonia concentration.

<https://doi.org/10.1371/journal.pone.0192217.g005>

proposed estimation method based on PF algorithm is more accurate for estimating the input ammonia concentration and can meet the actual needs.

As is mentioned above, the ammonia coverage ratio cannot be directly measured by a physical sensor. Thus, we can only compare the ammonia coverage ratio values between the SCR model and the designed observers. And Fig 8 presents the comparison of the SCR model

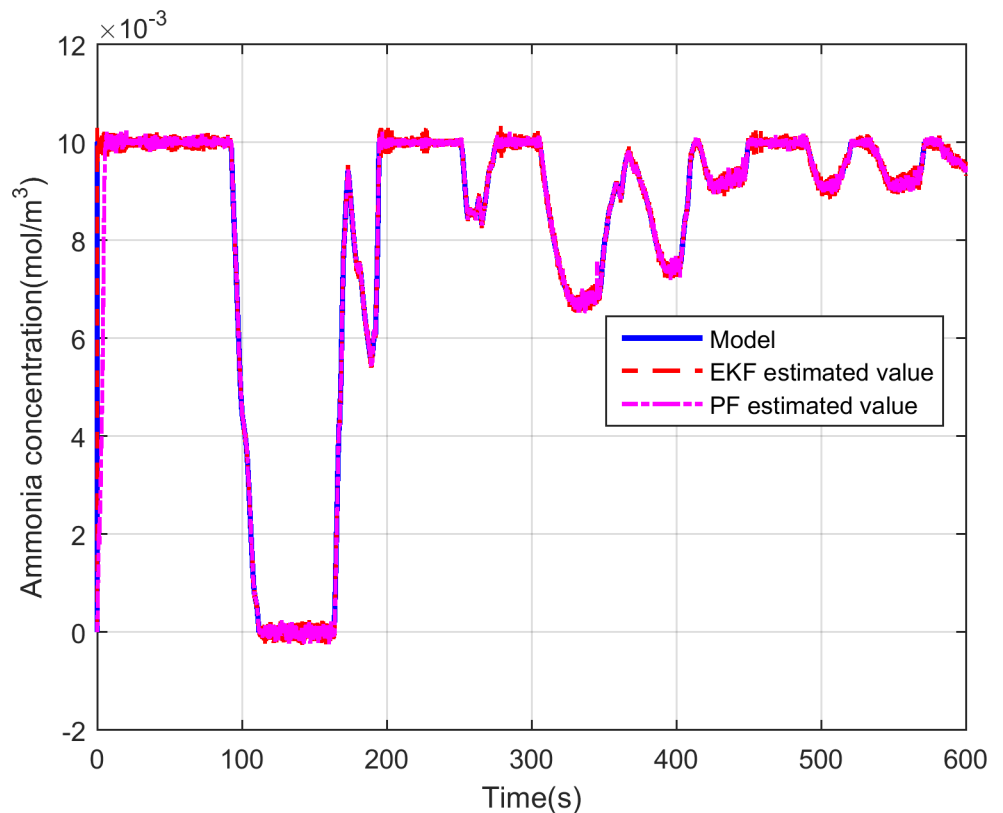


Fig 6. Comparisons of model predicted ammonia concentration and PF estimated ammonia concentration.

<https://doi.org/10.1371/journal.pone.0192217.g006>

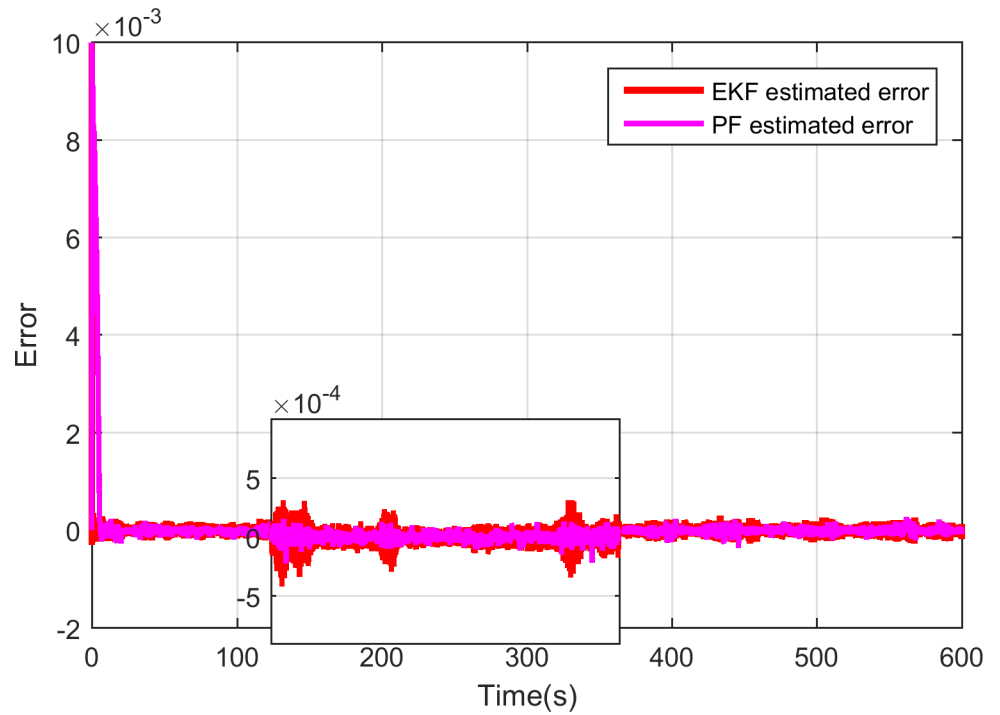


Fig 7. Errors of model predicted ammonia concentration and PF estimated ammonia concentration.

<https://doi.org/10.1371/journal.pone.0192217.g007>

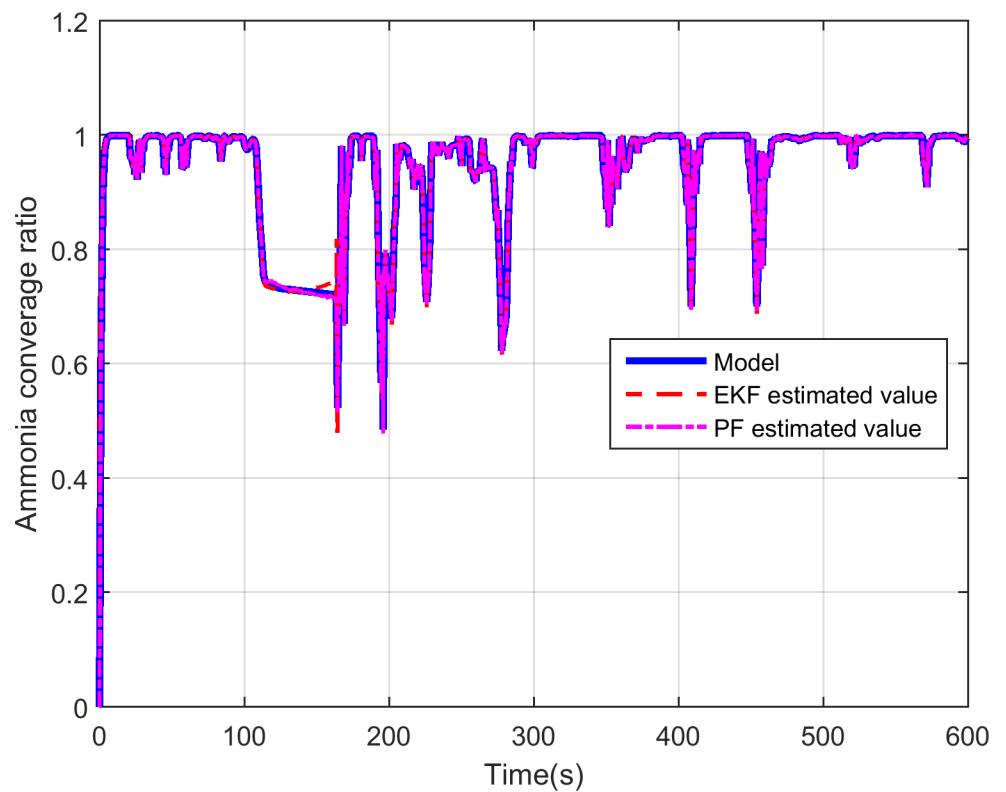


Fig 8. Comparison of model predicted ammonia coverage ratio and PF estimated ammonia coverage ratio.

<https://doi.org/10.1371/journal.pone.0192217.g008>

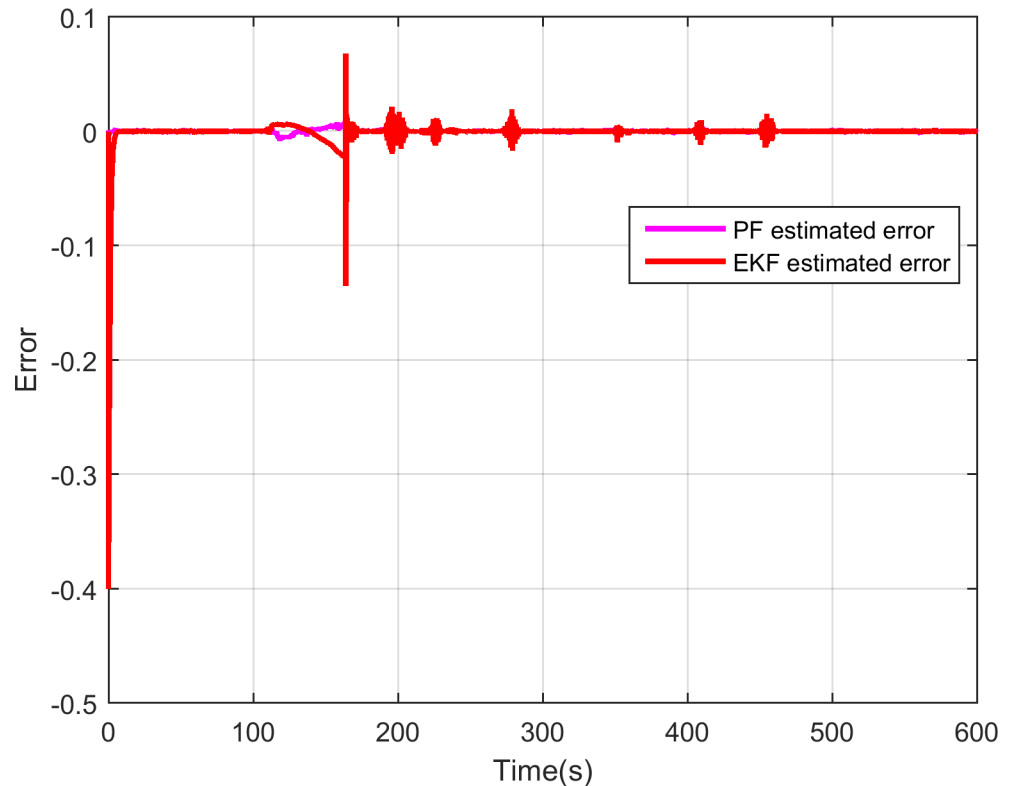


Fig 9. Errors of model predicted ammonia coverage ratio and PF estimated ammonia coverage ratio.

<https://doi.org/10.1371/journal.pone.0192217.g009>

calculated ammonia coverage ratio and the estimated one by the developed EKF and PF observers where we can see that the estimated ammonia coverage ratio by PF observer can better approach to the one of the SCR model than the one by EKF, especially at around 180s. Fig 9 is the error, and the error is defined as the model calculated value minus the observer estimated value. As is shown in the figure, the errors induced by EKF observer are severe at some time. On the contrary, though the ammonia coverage ratio calculated by the SCR model changes violently, the PF observer can catch up with it quickly and the errors depicted in Fig 9 are quite small which shows the performance of the designed observer based on PF algorithm works better for the SCR system.

Conclusions

The PF observer for input ammonia concentration and ammonia coverage ratio estimations is studied in this paper. Though the input ammonia concentration value can be measured by ammonia sensors, this method will increase the cost and diagnosis challenge of the SCR device. Inspired by the problem, the PF observer is designed to replace the physical sensors. According to the comparison results, the performance of the designed observer based on PF is excellent during the FTP-75 test cycle. Therefore, with the assistance of the developed observer, the ammonia sensor placed at the entrance of the SCR tank can be cancelled. What's more, the ammonia coverage ratio information is critical in the construction of the feedback control strategy and cannot be measured directly by physical sensor. And the simulation results and comparisons show that the designed PF observer has a pretty good ability to estimate the ammonia coverage ratio value.

In the future research, more experiments for Diesel-engine and SCR system will be done gradually, and other kinds of estimation methods will be considered. Besides, the closed-loop control strategy based on ammonia coverage ratio and other crucial states will be designed.

Supporting information

S1 File. The data file.

(MAT)

Author Contributions

Conceptualization: Kangfeng Sun, Shichun Yang.

Funding acquisition: Shichun Yang.

Methodology: Kangfeng Sun, Fenzhu Ji.

Project administration: Xiaoyu Yan.

Software: Kangfeng Sun, Fenzhu Ji, Kai Jiang.

Validation: Kangfeng Sun, Fenzhu Ji, Kai Jiang.

Writing – original draft: Kangfeng Sun, Fenzhu Ji.

Writing – review & editing: Kangfeng Sun, Fenzhu Ji.

References

1. Chen P, Wang J, editors. Integrated diesel engine and selective catalytic reduction system active NO_x control for fuel economy improvement. American Control Conference; 2013.
2. Zhang H, Wang J. Ammonia coverage ratio and input simultaneous estimation in ground vehicle selective catalytic reduction (SCR) systems. *Journal of the Franklin Institute*. 2015; 352(2):708–23.
3. Zhang H, Wang J, Wang YY. Robust Filtering for Ammonia Coverage Estimation in Diesel Engine Selective Catalytic Reduction (SCR) Systems. *Journal of Dynamic Systems Measurement & Control*. 2013; 135(6):1012–30.
4. Hsieh MF, Wang J. NO and NO₂ Concentration Modeling and Observer-Based Estimation Across a Diesel Engine Aftertreatment System. *Journal of Dynamic Systems Measurement & Control*. 2011; 133(4):041005.
5. Johnson TV. Review of Diesel Emissions and Control. *International Journal of Engine Research*. 2010; 10(5):275–85.
6. Bidarvatan M, Shahbakhti M. Integrated HCCI Engine Control based on a Performance Index. *Journal of Engineering for Gas Turbines & Power*. 2013; 136(10):V001T05A7.
7. Pournazeri M, Khajepour A, Huang Y. Development of a new fully flexible hydraulic variable valve actuation system for engines using rotary spool valves. *Mechatronics*. 2017; 46:1–20.
8. Wang J. Hybrid Robust Air-Path Control for Diesel Engines Operating Conventional and Low Temperature Combustion Modes. *IEEE Transactions on Control Systems Technology*. 2008; 16(6):1138–51.
9. Koebel M, Elsener M, Kleemann M. Urea-SCR: a promising technique to reduce NO_x emissions from automotive diesel engines. *Catalysis Today*. 2000; 59(3):335–45.
10. Wang J, Chia A, Menq H, Rizzoni G, Yurkovich S. CONTROL OF DIESEL ENGINE UREA SELECTIVE CATALYTIC REDUCTION SYSTEMS. Etdohiolinkedu. 2010.
11. Willems F, Cloudt R, Eijnden EVD, Genderen MV, Verbeek R, Jager BD, et al., editors. Is closed-loop SCR control required to meet future emission targets?2007.
12. Hsieh MF, Wang J. A Two-Cell Backstepping-Based Control Strategy for Diesel Engine Selective Catalytic Reduction Systems. *IEEE Transactions on Control Systems Technology*. 2011; 19(6):1504–15.
13. Zhang H, Chen Y, Wang J, Yang S. Cycle-based optimal NO_x emission control of selective catalytic reduction systems with dynamic programming algorithm. *Fuel*. 2015; 141:200–6.

14. Hsieh MF, Wang J. Adaptive and Efficient Ammonia Storage Distribution Control for a Two-Catalyst Selective Catalytic Reduction System. *Journal of Dynamic Systems Measurement & Control*. 2012; 134(1):011012.
15. Zhang H, Wang J, Wang YY. Nonlinear Observer Design of Diesel Engine Selective Catalytic Reduction Systems With NO_x Sensor Measurements. *IEEE/ASME Transactions on Mechatronics*. 2015; 20(4):1585–94.
16. Zhang H, Wang J, Wang YY. Sensor Reduction in Diesel Engine Two-Cell Selective Catalytic Reduction (SCR) Systems for Automotive Applications. *IEEE/ASME Transactions on Mechatronics*. 2015; 20(5):2222–33.
17. Kalman RE. A New Approach to Linear Filtering and Prediction Problems. *Journal of Basic Engineering Transactions*. 1960; 82:35–45.
18. Luenberger DG. Observing the State of a Linear System. *Military Electronics IEEE Transactions on*. 2007; 8(2):74–80.
19. Wang Y, Zhang C, Chen Z. On-line battery state-of-charge estimation based on an integrated estimator. *Applied Energy*. 2015; 185:2026–32.
20. Shenoy AV, Prasad V, Shah SL. Comparison of unconstrained nonlinear state estimation techniques on a MMA polymer reactor. *IFAC Proceedings Volumes*. 2010; 43(5):159–64.
21. Mallick M, Marrs A, editors. Comparison of the KF and particle filter based out-of-sequence measurement filtering algorithms. *Information Fusion, 2003 Proceedings of the Sixth International Conference of*; 2003.
22. Won SHP, Melek WW, Golnaraghi F. A Kalman/Particle Filter-Based Position and Orientation Estimation Method Using a Position Sensor/Inertial Measurement Unit Hybrid System. *IEEE Transactions on Industrial Electronics*. 2010; 57(5):1787–98.
23. Tulsyan A, Tsai Y, Gopaluni RB, Braatz RD. State-of-charge estimation in lithium-ion batteries: A particle filter approach. *Journal of Power Sources*. 2016; 331:208–23.
24. Wang Y, Zhang C, Chen Z. A method for state-of-charge estimation of LiFePO₄ batteries at dynamic currents and temperatures using particle filter. *Journal of Power Sources*. 2015; 279(ISSN):306–11.
25. Dong H, Jin X, Lou Y, Wang C. Lithium-ion battery state of health monitoring and remaining useful life prediction based on support vector regression-particle filter. *Journal of Power Sources*. 2014; 271:114–23.
26. Chi JN, Dacosta HFM. Modeling and Control of a Urea-SCR Aftertreatment System. *Sae Transactions*. 2005; 114(4):449–64.
27. Yim SD, Kim SJ, And JHB, Nam IS, Mok YS, Lee JH, et al. Decomposition of Urea into NH₃ for the SCR Process. *Industrial & Engineering Chemistry Research*. 2004; 43(16):4856–63.
28. Tronconi E, Lietti L, Forzatti P, Malloggi S. Experimental and theoretical investigation of the dynamics of the SCR—DeNO_x reaction. *Chemical Engineering Science*. 1996; 51(11):2965–70.
29. Devarakonda M, Parker G, Johnson JH, Strots V, Santhanam S, editors. Adequacy of Reduced Order Models for Model-Based Control in a Urea-SCR Aftertreatment System. *SAE World Congress & Exhibition*; 2008.
30. Cao E, Jiang K. Adaptive unscented Kalman filter for input estimations in Diesel-engine selective catalytic reduction systems. *Neurocomputing*. 2016; 205(C):329–35.
31. Meisami-Azad M, Mohammadpour J, Grigoriadis KM, Harold MP, Franchek MA. LPV gain-scheduled control of SCR aftertreatment systems. *International Journal of Control*. 2012; 85(1):114–33.
32. Upadhyay D, Nieuwstadt MV. Model Based Analysis and Control Design of a Urea-SCR deNO_x Aftertreatment System. *Journal of Dynamic Systems Measurement & Control*. 2006; 128(3):737–41.
33. Shao S, Bi J, Yang F, Guan W. On-line estimation of state-of-charge of Li-ion batteries in electric vehicle using the resampling particle filter. *Transportation Research Part D Transport & Environment*. 2014; 32(32):207–17.
34. Arulampalam MS, Maskell S, Gordon N, Clapp T. A tutorial on particle filters for online nonlinear/non-Gaussian Bayesian tracking. *IEEE Transactions on Signal Processing*. 2002; 50(2):174–88.
35. György K, Kelemen A, Dávid L. Unscented Kalman Filters and Particle Filter Methods for Nonlinear State Estimation. *Procedia Technology*. 2014; 12(1):65–74.
36. Ming FH, Wang J, editors. An extended Kalman filter for NO_x sensor ammonia cross-sensitivity elimination in selective catalytic reduction applications. *American Control Conference*; 2010.
37. Jiang K, Cao E, Wei L. NO_x sensor ammonia cross-sensitivity estimation with adaptive unscented Kalman filter for Diesel-engine selective catalytic reduction systems. *Fuel*. 2016; 165:185–92.
38. Jiang K, Geng P, Meng F, Zhang H. An extended Kalman filter for input estimations in diesel-engine selective catalytic reduction applications. *Neurocomputing*. 2016; 171(C):569–75.

39. Arnett M, Bayar K, Coburn C, Guezennec Y, Koprubasi K, Midlammohler S, et al. Cleaner Diesel Using Model-Based Design and Advanced Aftertreatment in a Student Competition Vehicle. 2008.
40. Song Q. Model-Based, Closed-Loop Control of Urea Scr Exhaust Aftertreatment System for Diesel Engine. Electronic Control Systems. 2002.